

In Vitro Study on the Synthesis of Seaweed *Ulva fasciata* Generated Nanoparticles and its Cytotoxicity Effect on Selected Continuous Cell Lines

ABSTRACT

Aim: To examine the effect of gold nanoparticles on normal Vero cell lines as well as on three different cancer cell lines (HepG2, HeLa, and MCF7) to evaluate their safety and toxicity. The study aims to assess the biocompatibility and potential cytotoxicity of gold nanoparticles, considering the ongoing debate about their effects on human health.

Study design: Experimental in vitro study.

Place and Duration of Study: This study was conducted at P.G. and Research Department of Biotechnology, Marudupandiyar college, Thanjavur

Methodology: In this study, *Ulva fasciata* seaweed was collected from coastal regions of Kerala and Tamil Nadu, cleaned, shade-dried, and powdered for methanolic extraction using Soxhlet apparatus. The resulting extract was used for the phytosynthesis of gold nanoparticles (Au NPs) by reacting with 1 mMHAuCl₄ under dark, static conditions at room temperature. Phytochemical screening identified various bioactive compounds in the extract. Optimization of nanoparticle synthesis was carried out by varying pH, temperature, extract and metal salt concentrations, and incubation time, with stability assessed over 12 months. The Au NPs were characterized using techniques such as UV-vis spectroscopy, HRTEM, EDX, XRD, DLS, zeta potential, AFM, and ICP-OES. Cytotoxic effects of the Au NPs were evaluated via MTT assay against normal (Vero) and cancer (HepG2, HeLa, MCF7) cell lines to determine IC₅₀ values, and apoptosis in HepG2 cells was confirmed using PI and AO/EB staining under fluorescence microscopy..

Results: Phytosynthesized gold nanoparticles (Au NPs) using *Ulva fasciata* extract exhibited a characteristic UV-Vis absorbance peak at 545 nm, confirming their formation. Phytochemical analysis of the extract revealed the presence of various bioactive compounds such as alkaloids, phenolics, flavonoids, and terpenoids, which likely mediated the nanoparticle synthesis. Optimal synthesis conditions were determined as pH 7, 1.0 mM HAuCl₄, 1.0 mL extract, 37 °C, and 24-hour incubation. Characterization revealed predominantly spherical, crystalline Au NPs with a size range of 25–35 nm by HR-TEM, a maximum hydrodynamic diameter of 50 nm (DLS), and a zeta potential of -16.0 mV, indicating good stability. XRD confirmed face-centered cubic structures, and EDX and SAED affirmed elemental purity and crystallinity. AFM showed smooth, spherical particles (~60–90 nm), and ICP-OES quantified Au NP concentration at 258.0 mg/L. In vitro cytotoxicity tests demonstrated higher biocompatibility of Au NPs (IC₅₀: 75 µg/mL) compared to gold chloride (IC₅₀: 10 µg/mL) in Vero cells. Au NPs showed dose-dependent anticancer activity, with IC₅₀ values of 30 µg/mL (HepG2) and 50 µg/mL (HeLa and MCF7). Fluorescent staining of HepG2 cells revealed apoptotic features, including chromatin condensation and nuclear fragmentation, confirming the pro-apoptotic effects of the Au NPs.

Conclusion: Gold nanoparticles show promise as a non-toxic drug delivery vehicle in normal cells while exhibiting cytotoxic effects in cancer cell lines. These findings suggest potential for selective therapeutic applications, though further studies are needed to confirm long-term safety and efficacy.

Keywords: Gold nanoparticles, *Ulva fasciata*, phytosynthesis, cytotoxicity, anticancer activity, characterization

1. INTRODUCTION

Nanoscience and nanotechnology are considered as key technologies for the current century. In nanotechnology, a particle is defined as a small object that behaves as a whole unit in terms of its transport and properties. Nanotechnology is characterized as the control of particles with no less than one size aspect measured between 1 to 100 nm measured in the range of 10^{-9} m. Nanoparticles are usually referred to as particles in the range of 1 - 100 nm. With the progression of nanotechnology, nanomaterials received substantial recognition in some fields like in environmental remediation and in medicines because they have distinctive property and characteristics like reactive oxygen species (ROS) production in cells, Inducement of apoptosis with cytotoxic, anticancer and antimicrobial properties and therefore used as drug carriers in human therapeutics. Over the past decade, several delivery vehicles have been designed based on different nanomaterials, such as polymers (Kisak *et al.*,2004), liposome (Wu *et al.*,2005), nanotubes (Salem *et al.*,2003) and nanorods (Brown *et al.*,2010). The large surface area / volume ratio of metal nanoparticles enables their surface to be coated with hundreds of molecules (including therapeutics, targeting agents and anti-fouling polymers) (Ghosh *et al.*,2008). Therapeutic vectors can carry drugs, genes and imaging agents into living cells and tissues (Edlund and Albertsson, 2003) provided that they must be safe for the host ecosystem.

There are different physical and chemical methods have been applied to synthesize the nanoparticles. However biological method is more significant due to easy accessibility because physical and chemical method for production and synthesis of nanoparticles greatly exposes its harmful hazardous effects on environment and human health predominately either by accidental or occupational exposure of harmful chemicals and reactants used during nanoparticle synthesis process. Whereas biological nanoparticle synthesis methods commonly known as Green synthesis methods include the use of bacteria, fungi and plants. The uses of plants have attracted more attention than the bacteria and fungi as they are easily available and do not require the maintenance of highly aseptic conditions (Sathishkumaret *al.*,2009). In recent years, plant mediated synthesis of nanoparticles is gaining importance as this method is facile and fast. *Medicago sativa* was the first plant to be reported for the synthesise of gold and silver nanoparticles (Torresdey *et al.*,2003). The therapeutic and diagnostic application of nanoparticles should not be toxic and must be biocompatible. Cytotoxicity of metal nanoparticles has been demonstrated by several research groups, since everything is toxic at an excess dose. The important question here is that whether metal nanoparticles are toxic or not at any specific concentration at which they can be used safely in the range of 1 to 100 nm (Shukla *et al.*,2005). Nanotoxicological studies are intended to determine whether and to what extent these nano properties may pose a threat to the environment and human beings. In this experiment, metal nanoparticles such as Gold nanoparticles (Au NPs) are biologically green synthesized from seaweed *Ulva fasciata* and along with other selected chemicals like gold chloride implemented over normal Vero cell lines and three selective cancer cell lines such as HepG2, HeLa and MCF7 for the study of their cytotoxic effects in correspondence to their different respective concentrations.

2. MATERIAL AND METHODS

2.1. Collection of Seaweed *Ulva fasciata*

Green seaweed *Ulva fasciata* was collected from the Indian coasts of Kerala and Tamil Nadu regions mainly from Kovalam, Mulloor and Muttom for the current study. They were immediately washed in fresh seawater to get rid of the epiphytes, sand, and other unwanted material. The alga was dried by air in the shade after the water had been drained off and soaked with a blotting sheet. They were cut into little pieces and subjected for drying at a temperature of 37°C in an incubator after finishing the shade drying procedure. A mechanical grinder was used to weigh and finely grind the fully dry material.

2.2. Isolation of secondary metabolites from the seaweed

Commented [D1]: Use more up-to-date references.

Commented [D2]: The introduction is written very briefly. It should be more complete.

Commented [D3]: Use more up-to-date references.

Commented [D4]: The purpose of the study should be written.

Commented [D5]: Written code of ethics

Commented [D6]: Written reference

Commented [D7]: Write the herbarium code of the plant.

Commented [D8]: Written reference

To obtain the crude extract using methanol as the solvent, 10 g of finely powdered *Ulva fasciata* alga were packed in Whatman No. 1 filter paper and fed into the Soxhlet equipment. The solvent was extracted thrice with distilled methanol while being refluxed at the proper boiling point (65°C). Finally, the packed substance was taken out and concentrated to a volume of 5 to 10 mL. Consequently, obtained extract was stored in the refrigerator for future employment in consecutive research.

Commented [D9]: Written reference

2.3. Phytosynthesis of gold nanoparticles (Mubarak Ali *et al.*, 2011)

One millilitre of the extract was collected, then 9.0 millilitres each of 1.0 mM HAuCl₄ were added. The reaction was carried out for 24 hours under static conditions in the dark at room temperature, and any changes in colour were noted. Gold nanoparticles that were created from *Ulva fasciata* seaweed were further examined and confirmed between 300 and 700 nm using a UV-vis spectrophotometer (HITACHI U-2900).

2.4. Qualitative phytochemical screening of *Ulva fasciata* seaweed extract

To find various phytoconstituents in the seaweed extract, the following assays were run according to the following procedures mentioned below. Detection of Alkaloids (Evans, 1997)- Mayer's test (Evans, 1997), Wagner's test (Wagner, 1993), Hager's test (Wagner *et al.*, 1996); Detection of Carbohydrates (Ramakrishnan *et al.*, 1994)- Benedict's test; Detection of Glycosides- Modified Borntrager's test (Evans, 1997); Detection of Phenolic compounds- Ferric chloride test (Mace, 1963), Gelatin test (Evans, 1997); Detection of Tannins- Gelatin test; Detection of Flavonoids- Alkaline reagent test, Lead acetate test; Detection of Terpenoids- Salkowski test; Detection of Proteins and Amino acids- Biuret test (Gahan, 1984), Ninhydrin test (Yasuma and Ichikawa, 1953); Detection of Diterpenes- Copper acetate test; Detection of Saponins- Foam test (Kokate, 1999) etc.

2.5. Optimization of the Phytosynthesis of gold nanoparticles

In the test tubes followed by 9 mL each of HAuCl₄ were added to 1.0 mL of seaweed extract to create gold bio nanoparticles, respectively, thereafter test tubes were subjected to under various external parameters and conditions. Consequently, their stability was measured using an HITACHI U-2900 spectrophotometer between 300 and 700 nm. The various external parameters were applied and noted which includes Effect of different pH value (pH 4, 5, 6, 7, 8, 9 and 10) ; Effect of different concentrations of gold chloride- 9.0 mL of HAuCl₄ were added separately to 1.0 mL of the selected extracts at concentrations of 0.5 mM, 1 mM, 1.5 mM, 2 mM, 2.5 mM, and 3 mM; Effect of different concentrations of extracts for the synthesis of Au NPs, various extract amounts of 0.5 mL, 1 mL, 1.5 mL, 2 mL, 2.5 mL, and 3 mL were taken and produced up to 10 mL using 1.0 mM HAuCl₄, respectively; Effect of different Temperatures-At several temperatures, including 22°C, 27°C, 32°C, 37°C, 42°C, 47°C, and 52°C, gold nanoparticles were phytosynthesized; Effect of different durations on phytosynthesis of gold nanoparticles- Phytosynthesis of gold nanoparticles tested across time periods of 0 hours, 6 hours, 12 hours, 18 hours, and 24 hours; Stability of phytosynthesized gold nanoparticles- The samples of phytosynthesized Au NPs were stored at room temperature in the dark for a full year. Using the HITACHI U-2900, the stability of the samples was measured between 300 and 700 nm on the fifth, fifteenth day, first, second, sixth, and twelfth months.

2.6. Characterization of the gold nanoparticles

AuNPs of the newly selected *Ulva fasciata* test tube were subjected to characterization procedure for morphological and further studies for example, UV-visible spectroscopy, High Resolution Transmission Electron Microscopy (HRTEM), Energy Dispersive X-ray analysis (EDX), Selected area electron diffraction (SAED), X-ray Diffraction Studies (XRD), Dynamic Light Scattering (DLS), Zeta Potential measurement, Atomic force microscopy (AFM), Inductively Coupled Plasma Optical Emission Spectroscopy (ICP-OES) instrumentation etc.

Commented [D10]: Written reference

2.7. Chemicals and reagents

The Gibco (Grand Island, NY, USA) provided the Cell culture Dulbecco's Modified Eagle Medium (DMEM) and Fetal Bovine Serum (FBS), 0.25% Trypsin-EDTA. From Sigma-Aldrich (St Louis, MO, USA), we obtained streptomycin, penicillin, dimethyl sulfoxide (DMSO), 3-(4,5-dimethylthiazol-2-yl)-2,5-diphenyltetrazolium bromide (MTT), phosphate buffer, and fluorescent dyes such as acridine orange and ethidium bromide (AO/EB) with higher than 98% purity. From the Himedia Lab Pvt. Ltd. (Mumbai, India) chloroauric acid/gold chloride (HAuCl₄) were purchased.

2.8. Cell culture maintenance

The National Centre for Cell Sciences (NCCS), Pune, India, provided the Vero African green monkey kidney normal cell line, HepG2 hepatocellular carcinoma, HeLa cervical cancer, and MCF7 breast epithelial adenocarcinoma cancer cell line. In DMEM media supplemented with 10% (v/v) heat inactivated foetal bovine serum, 100 U/mL penicillin, and 100 g/mL streptomycin, cells were kept in the logarithmic phase of growth. They were kept at 37 °C in an incubator with 5% CO₂ and 95% humidified air.

2.9. Effect of phytosynthesized gold nanoparticles on cytotoxicity of cell lines – MTT assay. (Mossman, 1983)

Phytosynthesized Au NPs were tested by MTT (3-(4,5-dimethylthiazol-2-yl)-2,5- diphenyl tetrazolium bromide assay) against both normal cell line Vero and cancer cell lines such as HepG2, HeLa, and MCF7.

2.9.1. Cytotoxicity analysis against Vero (Normal) cell line. (Asra Parveen and Srinath Rao, 2015)

Prior to researching the anti-proliferative effect against cancer cell lines, it is critical to determine the drug and metal nanoparticle compatibility and dosage on normal cell lines. In the current work, the cytotoxic effects of various doses of gold chloride and gold nanoparticles (Au NPs) were investigated against the Vero cell line. The individual, viable Vero cells were planted at 1x10⁶ cells/mL in 96-well microplates and cultured at 37°C for 24 hours in a 5% CO₂ incubator. This allowed the cells to swell to 90% confluence. At the conclusion of the incubation, the medium was changed, and the Vero cells were treated with gold chloride and Au NPs at concentrations of 5, 10, 30, 50, 75, and 100 µg/mL. Incubation of the samples followed for 24 hours. The cells were then washed with phosphate-buffered saline (PBS, pH-7.4) and added 20µL of (MTT) solution (5 mg/mL) to each well and allowed to stand at 37°C in the dark for additional 4 h then added 100µL DMSO and dissolved the formazan crystals and its absorbance was read spectrometrically at 570 nm using ELISA plate reader. The fraction of viable cells was calculated.

2.9.2. Cytotoxicity analysis against cancer cell lines

Separately planted in 96-well microplates with 1x10⁶ cells per well, HepG2, HeLa, and MCF7 cell lines were cultured at 37°C for 24 hours in a 5% CO₂ incubator and allowed to reach 90% confluence. After changing the media, the cells were exposed to Au NPs at various concentrations, including 5, 10, 30, 50, 75, and 100 µg/mL, and incubated for 24 hours. After using phosphate-buffer saline (PBS, pH 7.4) to wash the cells, 20 µL of the MTT solution (5 mg/mL) was added to each well. After that, the plates were left at 37 °C in the dark for an additional 4 hours. The absorbance was measured spectrophotometrically at 570 nm after the formazan crystals were dissolved in 100 µL of DMSO. The formula above was used to express the fraction of viable cells.

The IC₅₀ value, a measure for cytotoxicity studies, was defined as the concentration that inhibited 50% of cell growth. After 24 hours, the morphological alterations of untreated (control) and IC₅₀-treated cells were examined under a bright field microscope and documented. HepG2 cells treated with phytosynthesized Au NPs demonstrated an IC₅₀ value of 30 µg/mL, whilst HeLa and MCF7 cells were each at 50 µg/mL after 24 hours. As the HepG2 cell line displayed a lower IC₅₀ value than the others, it was chosen for further research.

2.10. Assessment of Apoptosis

2.10.1. Propidium iodide (PI) nucleic acid stain (Hirak et al., 2007)

HepG2 cells were plated in a six-well chamber plate at a density of 5×10^4 cells per well. The cells were exposed to phytosynthesized Au NPs for 24 hours after reaching > 90% confluence. The cells were then stained with 50 $\mu\text{g/mL}$ propidium iodide (PI) for 20 minutes after being rinsed with PBS and fixed in a 3:1 mixture of methanol and acetic acid for 10 minutes. Fluorescent microscopy called FLoid Cell Imaging was used to analyse the nuclear morphology of apoptotic cells.

2.10.2. Determination of mode of cell death by acridine orange (AO) / ethidium bromide (EB) dual staining (Jeyaraj et al., 2013)

HepG2 cells were plated in 6-well plates and exposed to Au NPs at the IC_{50} concentration for 24 hours. The monolayer of cells was rinsed with PBS before being stained with 5 μL of acridine orange (100 $\mu\text{g/mL}$) and 5 μL of ethidium bromide (100 $\mu\text{g/mL}$) for the nuclear examination. FLoid Cell Imaging fluorescent microscopy was used to detect the morphological changes in the stained cells and the apoptotic nuclei (intensely stained, fragmented nuclei, and condensed chromatin).

3. RESULTS

3.1. Phytosynthesis of gold nanoparticles

The reduction of Au NPs (545 nm) in the solution of gold complex during the reaction with the seaweed extracts of *Ulva fasciata* was confirmed by the UV-vis spectra.

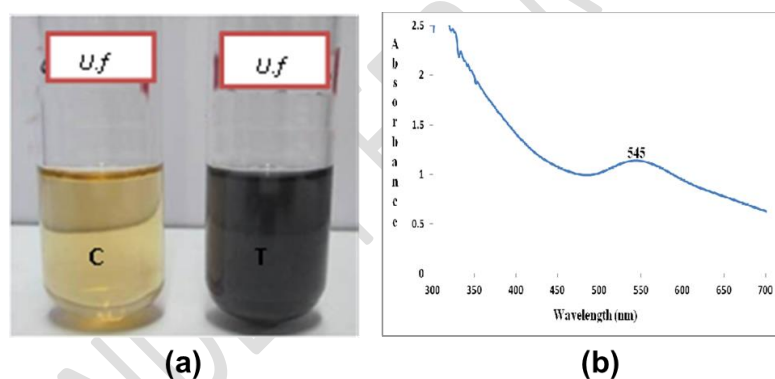


Fig. 1. Synthesis and UV Characterization of the Phytosynthesized Gold nanoparticle

(a) Color change in phytosynthesized Au NP (b) UV-visible spectroscopy of Au NP

3.2. Qualitative phytochemical analysis of crude seaweed extract of *Ulva fasciata*

The seaweed extracts of *Ulva fasciata* showed the presence of alkaloids (positive for Mayer's test, Wagner's test, Hager's test), carbohydrates (positive for Benedict's test), glycosides (positive for Modified Borntrager's test), phenolic compounds (positive for Ferric chloride test, Gelatin test), proteins, amino acids (positive for Biuret reagent, Ninhydrin reagent), flavonoids (positive for Alkaline reagent test, Lead acetate test), terpenoids (positive for Salkowski test) and Saponins (negative for foam test).

3.3. Optimization of the phytosynthesized gold nanoparticles from *Ulva fasciata*

The stability of phytosynthesized gold nanoparticles were high and at the peak when the selected solution test tube consists of optimum external parameters such as pH 7 (530 nm); 1.0 mM HAuCl₄ concentration (530 nm); 1.0 mL of *Ulva fasciata* extract (530 nm); 37°C temperature (545 nm) and stability up to 24-hour timing (530 nm).

3.4. Characterization of Gold Nanoparticles

3.4.1. High resolution transmission electron microscopy

The particles size, distribution, shape and morphology of Au NPs were characterized using HR-TEM showed Au NPs were predominantly spherical in shape with an average particle size of 25 - 35 nm.

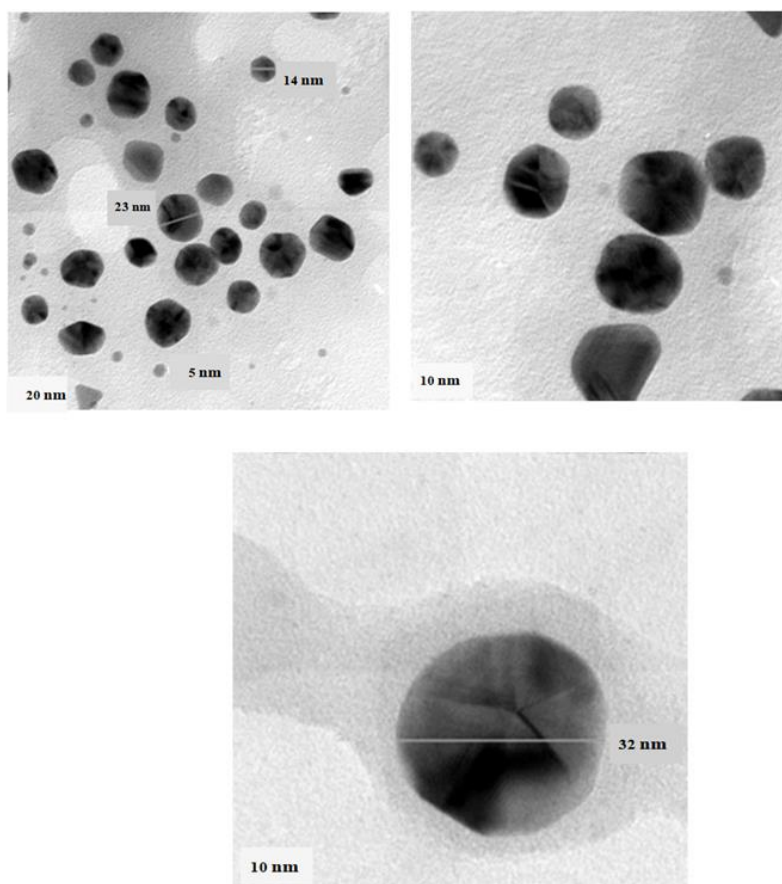


Fig. 2.High resolution transmission electron microscope of Au NPs synthesized from *Ulva fasciata*

3.4.2. Energy dispersive X-ray analysis

The EDX spectra displayed a single signal for gold nanoparticles indicating that the synthesized NPs were free from impurities; The presence of O and C peaks over the Au signals indicates that phytoconstituents used oxygen atoms to cap the Au NPs.

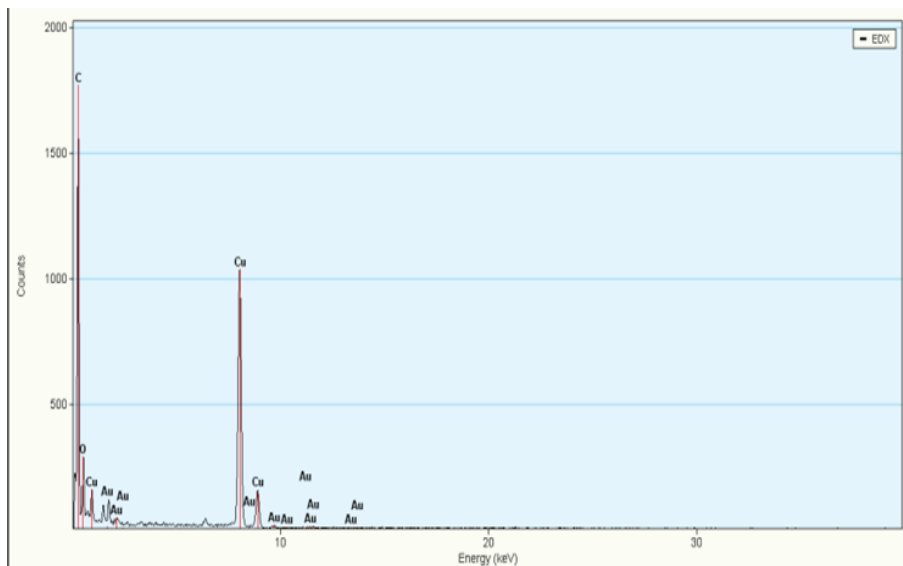


Fig.3. Energy dispersive X-ray analysis of phytosynthesized Au NPs

3.4.3. Selected area electron diffraction (SAED)

The selected area electron diffraction (SAED) spectra confirmed that the Au NPs synthesized are crystalline in nature;

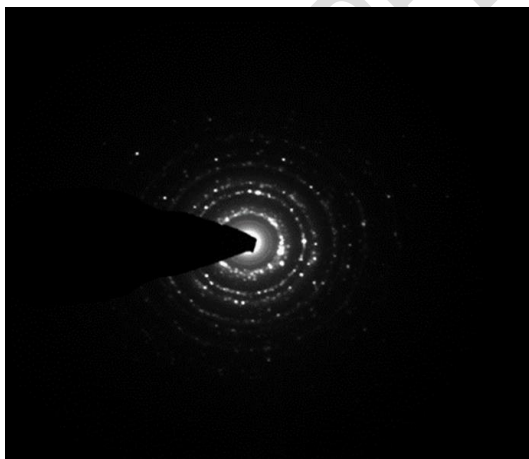


Fig.4. Selected area electron diffraction of phytosynthesized Au NPs

3.4.4. X-ray Diffraction pattern analysis

In XRD pattern, the peaks of gold recorded at $2\theta = 38.0^\circ$, 44.2° , 64.4° confirmed the purity of the samples. The sharp peak displays the crystalline nature of Au NPs and corresponding hkl planes are (111), (200), (220). This plane represents the face-centered cubic (fcc) structure of the Au NPs in comparison with standard JCPDS file number 65-2870. The crystallite size of Au NPs was calculated using Scherrer formula confirmed the presence of Nano crystalline Au.

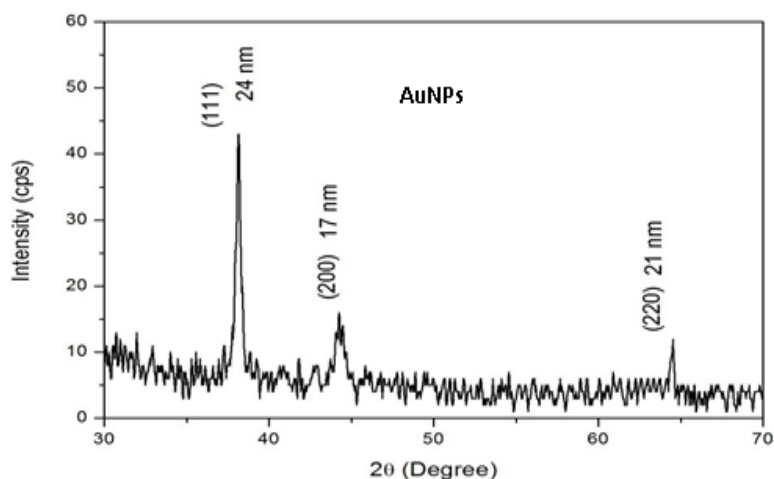


Fig.5. X-ray diffraction analysis of Au NPs synthesized from *Ulva fasciata*

3.4.5. Dynamic light scattering (DLS)

DLS analysis shows the hydrodynamic diameter using the auto correlation function and the diffusion coefficient of the mono-dispersive colloids containing Au NPs. They showed maximum size of 50 nm for Au NPs, respectively.

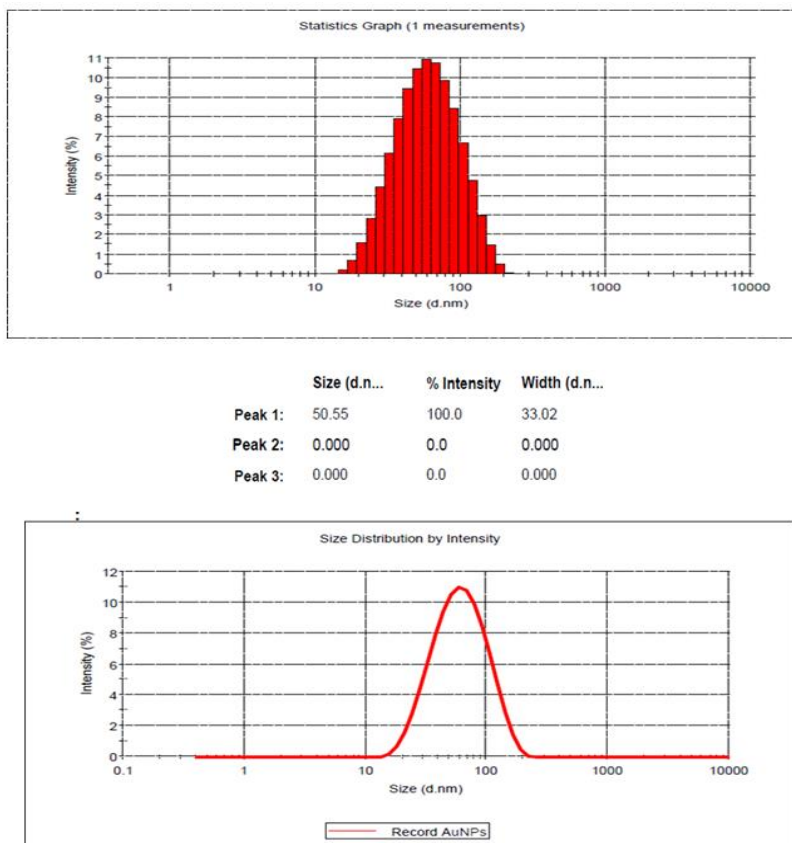


Fig.6. Dynamic light scattering of Au NPs synthesized from *Ulva fasciata*

3.4.6. Zeta potential analysis

The zeta potential is found to be -16.0 mV for Au NPs, respectively. The negative value in specific may be due to the bio-organic compounds capped on the nanoparticles. The negative charge intensity indicates that the Au NPs are found stable.

	Mean (mV)	Area (%)	Width (mV)
Zeta Potential (mV): -16.0	Peak 1: -16.0	100.0	4.65
Zeta Deviation (mV): 4.65	Peak 2: 0.00	0.0	0.00
Conductivity (mS/cm): 1.30	Peak 3: 0.00	0.0	0.00
Result quality : Good			

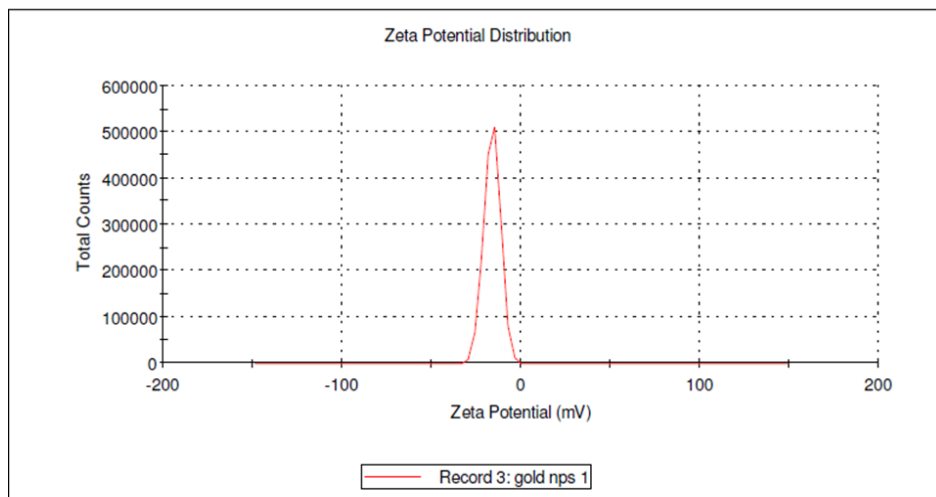


Fig.7. Zeta potential of Au NPs synthesized from *Ulva fasciata*

3.4.7. Atomic force microscopy (AFM) & Inductively plasma optical emission spectroscopy (ICP-OES)

Surface morphology of the metal nanoparticles was studied under AFM as for Au NPs, respectively. The size of the particles was in the range of ~60-90 nm for Au NPs, respectively. Gold were displaying spherical shape of nanoparticles with smooth surface, without any pinholes or cracks. The phytosynthesized Au NPs were quantitatively determined by ICP- OES analysis which showed that the concentration of AuNPs were and 258.0 mg/L, respectively. The elemental wavelength of Au NPs was 267.595, respectively.

3.5. Cytotoxicity analysis against Vero (Normal) cell line-MTT assay

The MTT assay was used to test the cytotoxicity of different concentrations of gold chloride, phytosynthesized Au NPs on Vero cells (a normal cell line) *in vitro*. Au NPs among them demonstrated a maximum with IC₅₀ value of 75 µg/mL, next was gold chloride, and with IC₅₀ values of 10 µg/mL, respectively. The salts of HAuCl₄ were less biocompatible than the Au NPs tested in Vero cells. Lower cell viability was seen in treated concentrations when compared to control ($p < 0.05$) in a significant manner.

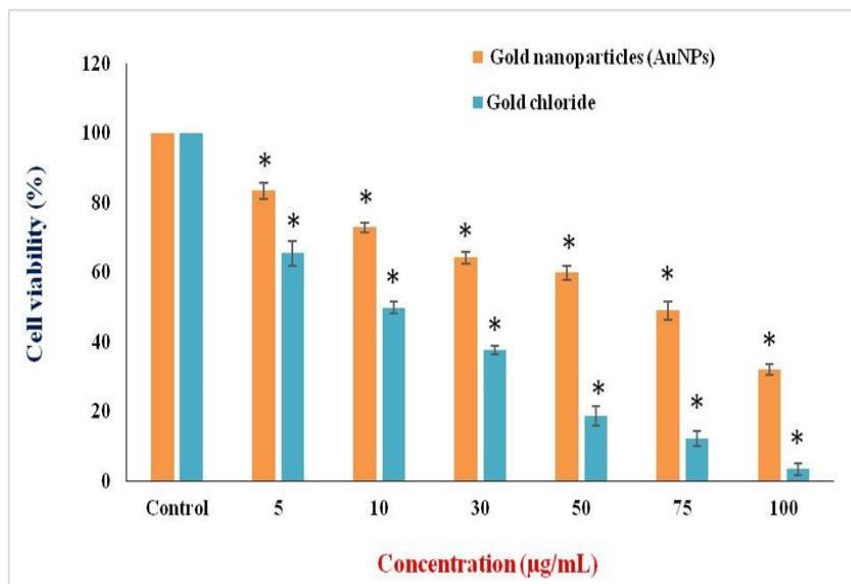


Fig.8. Effect of different concentration of HAuCl_4 and phytosynthesized Au NPs on Vero cell line at 24 h. Values are given as mean \pm S.D for each concentration. The treated concentrations statistically significant ($p < 0.05$) when compared to control.

Commented [D11]: What does the asterisk mean in the subtitles?

3.5.1. Morphological observation of Vero cells

The Vero cells were exposed for 24 hours to the IC_{50} concentrations of gold chloride, and gold nanoparticles, and the results showed that the cells rounded, shrank, and lost contact with surrounding cells. The materials' harmful effects on Vero cells were confirmed by the images.

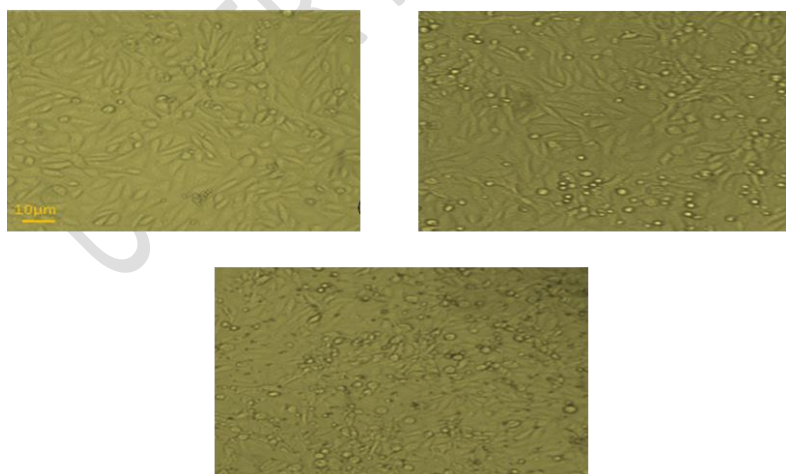


Fig.9. Effect of HAuCl_4 and Au NPs on Vero cell line at 24 h

(a) Control (b) Au NPs treated (75µg/mL) (c) H₂SO₄ treated (10µg/mL).

3.6. Cytotoxicity for phytosynthesized AuNPs against cancer cell lines

The MTT assay was used to evaluate the anti-proliferative effects of Au NPs on three different cell lines, including HepG2, HeLa, and MCF7 cells. Au NPs antagonistic procedures were dose-dependent mechanisms on HepG2, HeLa, and MCF7 cells at doses of 5, 10, 30, 50, 75, and 100 µg/mL. HepG2 cells had an inhibitory concentration of IC₅₀ of 30 µg/mL, but HeLa and MCF7 cells had an inhibitory concentration of 50 µg/mL each after 24 hours. Lower cell viability was seen in treated concentrations when compared to control ($p < 0.05$) in a significant manner.

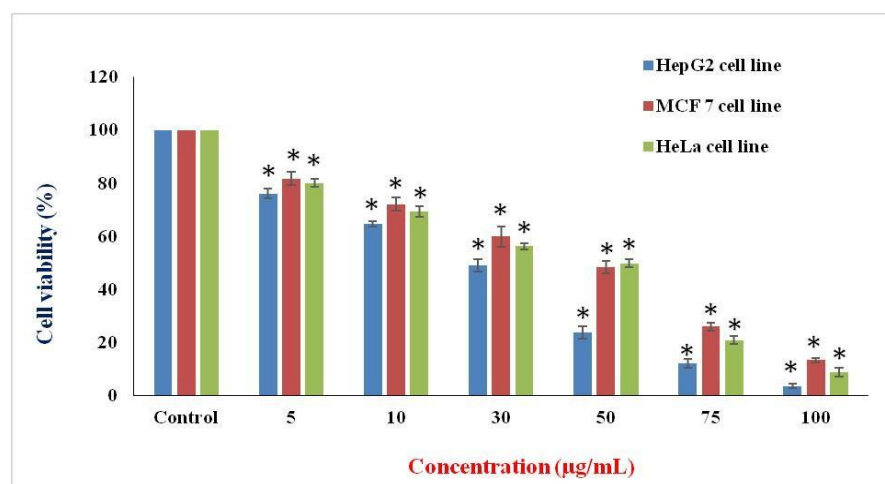


Fig.10. Effect of different concentration of Au NPs on HepG2, MCF7 and HeLa cell lines at 24 h. Values are given as mean \pm S.D for each concentration. The treated concentrations statistically significant ($p < 0.05$) when compared to control.

3.6.1. Morphological observations

HepG2 cells were discovered in irregular confluent aggregates that were rounded and polygonal after being exposed to AuNPs at an IC₅₀ of 30 µg/mL for 24 hours. The cells had a lot of protrusions on their surfaces. Condensed plasma membrane was discovered. Under the nuclear membrane, a substantial quantity of nuclear chromatin aggregation was seen.

Commented [D12]: What does the asterisk mean in the subtitles?

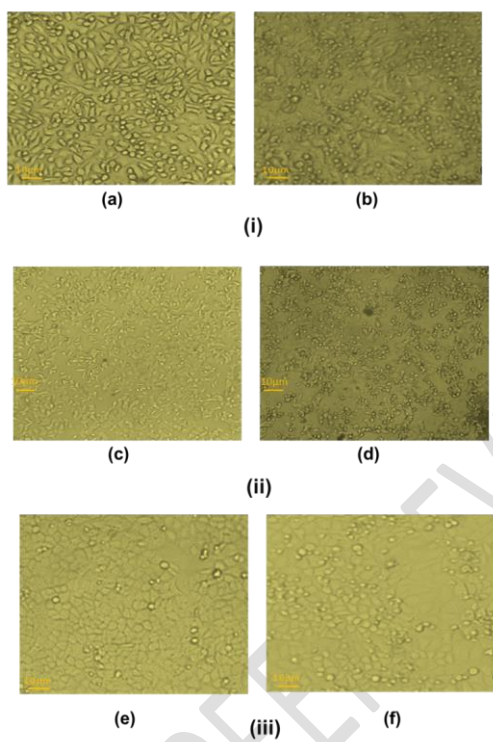


Fig 11. Cytotoxicity effect of AuNP against different cancer cell line

(i) Effect of AuNPs on HepG2 cells at 24h; (a) Control (b) Au NPs treated (30µg/mL); (ii) Effect of AuNPs on MCF7 cells at 24h; (a) Control (b) Au NPs treated (50µg/mL); (iii) Effect of AuNPs on HeLa cells at 24h; (a) Control (b) Au NPs treated (50µg/mL)

3.6.2. Morphological features of HepG2 cells stained with propidium iodide under fluorescence microscope

After 24 hours, the morphological characteristics of HepG2 treated with IC₅₀ concentrations of Au NPs revealed condensation and fragmentation of dead cells.

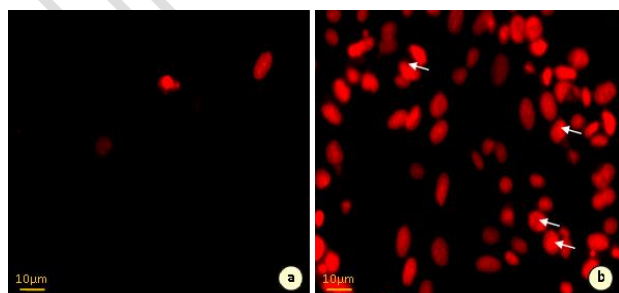


Fig.12. Morphological features of HepG2 cells stained with propidium iodide under fluorescence microscope

(a.) HepG2 control cells (b.) Au NPs treated cells.

3.6.3. Morphological features of HepG2 cells double stained with acridine orange / ethidium bromide under fluorescence microscopy

In comparison to untreated control cells, HepG2 cells treated with IC_{50} concentrations of Au NPs displayed morphological apoptotic alterations when stained with acridine orange/ethidium bromide (AO/EB) fluorescence staining after 24 hours. The cytoplasm and nuclei of the control cells had been uniformly brilliant green. However, the Au NP-treated cells displayed the telltale signs of death, including cell shrinkage, nuclear condensation and fragmentation, and the development of apoptotic bodies.

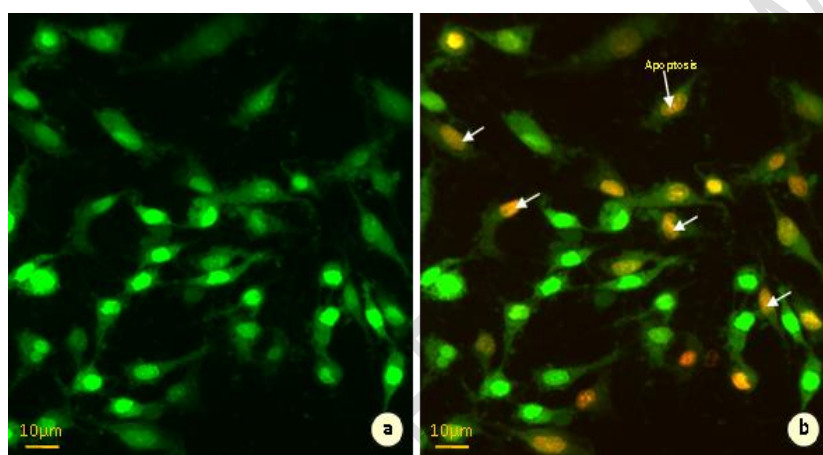


Fig.13. Effect of Au NPs at 30µg/mL on nuclei of HepG2 cells at 24h-stained with acridine orange and ethidium bromide.

(a.) HepG2 control cells (b.) Au NPs treated cells

4. DISCUSSION

In industrial, medicinal, and biological uses, silver and gold nanoparticles are crucial. Recent years have seen extensive research into the development of medication delivery systems that can successfully elicit the intended therapeutic effect in patients with little unwanted responses (Khan *et al.*, 2014). Cell viability and cytotoxicity are the main factors used to assess the biocompatibility of gold nanoparticles. The MTT assay was used to assess the cytotoxicity of Au NPs *in vitro* on Vero cells in terms of how they affected cell growth.

Gold is a multifunctional material that has been utilized in medicinal applications for centuries because it has been recognized for its substantial properties. Modern medicine is regularly trying to routine and conventional use of gold and has even developed more advanced applications by taking advantage of its ability to be manufactured at the nanoscale and particularly functionalization due to the reason of the availability of thiol and amine groups, allowing for the conjugation of various functional groups such as targeted antibodies or drug products. It has been demonstrated that colloidal gold exhibits localized Plasmon surface resonance (LPSR) effect, meaning that gold nanoparticles can absorb light at specific wavelengths, resulting in photoacoustic and photothermal characteristics, making them potentially useful for hyperthermic cancer treatments and imaging applications. Modifying and formulating gold nanoparticle shape and size can effectively change their LPSR photochemical activities, thereby also altering their photothermal and photoacoustic properties,

Commented [D13]: Write down the possible mechanism of the results obtained.

allowing for the utilization of different wavelengths of light, for instance as light in the near-infrared spectrum. By manufacturing gold in a nanoscale format, it is possible to passively distribute the material inside the body, where it can localize in tumors and be safely excreted through the urinary system (Vines *et al.*, (2019).

Several studies have documented the *in vitro* anticancer efficacy of plant-mediated Au NPs on various cancer cell lines, including lung, breast, prostate, colon, and ovarian cancer. Au NPs nanoparticles have demonstrated therapeutic effects by inhibiting cell growth, causing cell cycle arrest, inducing apoptosis, and blocking various signaling pathways essential for tumor development. Simultaneously, it is a safe and targeted method for cancer therapy because of their special physicochemical characteristics, such as high surface area-to-volume ratio, biocompatibility, and capacity to be functionalized with different targeted molecules. Along with their small size, they have improved permeability and retention (EPR) in tumor tissues, which improves therapeutic efficacy, decrease systemic toxicity, and enables for targeted drug administration (Nisha *et al.*, (2024).

AuNPs can efficiently absorb visible, UV, and NIR light and release energy as heat. The ability to functionalize Au NPs surface with targeting moieties allows for their selective delivery to cancer sites with exciting potential. Numerous chemotherapeutic drugs—including Paclitaxel (PTX), 5-fluorouracil (5-FU) and Gemcitabine (GMC)—have been conjugated with Au NPs to reduce dose quantity and the side effects of treatment. It has also been established that Methotrexate (MTX) or Doxorubicin (DOX) conjugated-Au NPs demonstrate higher levels of cytotoxicity and better accumulation in tumor cells than free MTX or DOX. However, even though the high number of gold nanomaterials developed there are persistent translation challenges with Au NPs. In fact, although Au NPs show potentially useful properties in many preclinical studies, there are very few clinical trials assessing the use of Au NPs for tumor diagnostics and therapy, and, to date, no preparations containing Au NPs have been used effectively in clinical practice. CYT-6091 (Aurimune) was the first product in clinical trials using Au NPs functionalized with the recombinant human tumor necrosis factor alpha for patients with advanced solid tumors (ClinicalTrials.gov Identifier: NCT00356980, NCT00436410). AuroShell, a silica-gold core-shell nanoparticle, is another example of Au NPs undergoing clinical trials for thermal ablation of localized tumors (NCT00848042, NCT01679470). Another formulation under clinical investigation is a NU-0129, a spherical nucleic acid (SNA) Au NPs, as a treatment for patients with recurrent glioblastomamultiforme or gliosarcoma (NCT03020017). Moreover, that an understanding of fundamental signal modulations induced by Au NPs at molecular and cellular levels may help to overcome persistent problems in nanomedicine and lead to Au NPs' clinical applications (Bloise *et al.*, (2022).

The diverse range of uses of gold nanoparticles across numerous disciplines, focusing on their distinctive characteristics in catalysis, optical properties, thermal conductivity, electrical conductivity, biological and environmental interactions. Nevertheless, there arises notable challenges too, including apprehensions over toxicity, the influence of nanoparticle size, and potential environmental repercussions. Notwithstanding these obstacles, the profound influence of gold nanoparticles in diverse domains such as environmental monitoring, renewable energy, catalysis, renewable energy, healthcare, cosmetics, and biotechnology. This highlights their capacity to mold the future through inventive and adaptable means (Hossain *et al.*, (2024).

Ovarian cancer is one the deadliest disease because the survival rate is very low. Even though the medical sciences have advanced much in recent years, research and researchers are still at the stage of infancy since patients are succumbing to this malignancy. Multidrug resistance, toxicity, mode of treatment problems like catheter related complication & issues poises a number of challenges to scientists worldwide. Novel therapy is now thus being used to sensitize the cells more towards the treatment. Gold nanoparticles (Au NPs), popular for their high biocompatibility, and strong optical & magnetic responses, have emerged as promising agents for both the diagnosis and treatment of ovarian cancer. Due to their physical characteristics, Au NPs may be used as adjuvants in radiotherapy, fluorescence imaging and bioimaging thus support the role of Au NPs in biological domains (due to strong surface plasmon resonance (SPR) properties, enhancing imaging techniques for early detection of ovarian tumors). Moreover, chemical properties such as Magnetic Resonance and Imaging Properties, X-ray imaging property, Two-photon or multiphoton imaging, and Optical coherence tomography (OCT) imaging properties enhance and encourage the use of Au NPs in diagnostic field. (Aggarwal *et al.*, (2025).

Vero cells were tested for cell survival after being exposed to phytosynthesized Au NPs at concentrations of 10, 50, 100, 150, and 200 μM nanoparticles for 24, 48, 72, and 96 hours. More than 85 to 90% of the cells exhibited viability at doses up to 150 μM . The biocompatibility rose with increasing incubation time, reaching 95 to 99% in all concentrations examined, demonstrating the Vero cells' adaption to the Au NPs environment (Jayshree *et al.*, 2012). According to Verma *et al.*, (2013), the Vero cell lines demonstrated considerable cell death at higher doses.

In the current study, the impact of various concentrations of gold chloride, and synthetically produced Au NPs under *in vitro* conditions on Vero cells. The largest IC_{50} value among them was 75 $\mu\text{g/mL}$ for Au NPs, followed by 10 $\mu\text{g/mL}$ for gold chloride respectively. The current attempt's cell viability assay revealed that Au NPs are less harmful than the rest. Au NPs eventually become more biocompatible over time at all concentrations. There are two theories for how metal NPs interact and are metabolised: the first is that adsorption causes growth to be delayed, and the second is that metabolism or internalisation leads to cell survival and healthy growth. According to this theory, Au NPs do not have a long-term detrimental effect on cell growth or survival. Due to their cytocompatibility, stability, and ease of binding with biomolecules, Au NPs in nanomedicine can be excellent nanocarriers of anti-cancer medications (Jiang *et al.*, 2008). Moreover, because of their visible-light scattering characteristics, they can function as molecular imaging agents on their alone or in combination with other fluorophores (Boisselier and Astruc, 2009). According to Mohammadi *et al.*, (2013), MCF7 and HepG2 cell lines were found to be cytotoxic to Au NPs at varied doses of 0, 1, 2, 4, and 8 mg/mL after 24 hours. Au NPs at 8 mg/mL caused 53.5% and 91.8% of the cells in MCF7 and HepG2 to die, respectively. For the MCF7 and HepG2 cell lines, the IC_{50} of the Au NPs was determined to be 6.82 and 2.90 mg/mL , respectively ($P < 0.05$). The impact of Au NPs on the growth depression of MCF-7 and HepG-2 cells varied significantly by 95 percent ($P < 0.05$). In addition, Singh *et al.*, (2014) noted that the HepG2 cell's periphery, outside of the cell nucleus, had an asymmetric buildup (accumulation) of Au NPs. In compared to lung cancer cells at a dose of 144.16 nM , the aggregation of particles within the cytoplasm of liver cancer cells treated with an IC_{50} of 82.91 nM resulted in a 50% loss in cell viability. The A549 cell line's morphological modifications appeared to be less pronounced in the phase contrast microscopic image. After treatment with Au NPs, the degree of the cell's roundness—one of the traits of stressed cells—was assessed.

The MTT assay was used in the current work to measure the anti-proliferative effects of Au NPs on three different cancer cell lines, including HepG2, HeLa, and MCF7 cells. At varied concentrations: 5, 10, 30, 50, 75, and 100 $\mu\text{g/mL}$, dose-dependent suppression of Au NPs on HepG2, HeLa, and MCF7 cells was noted. HepG2 cells had an IC_{50} of 30 $\mu\text{g/mL}$, but HeLa and MCF7 cells both had an IC_{50} of 50 $\mu\text{g/mL}$ after 24 hours. Cell viability was seen to be significantly lower in treated concentrations as compared to controls ($p < 0.05$). Their findings showed that all cancer cell lines became more hazardous as Au NPs concentrations increased. When gold ions from gold nanoparticles interact with phosphorus moieties in DNA, DNA replication is inhibited. When gold ions engage with sulfur-containing proteins, enzyme functions are inhibited, which causes a loss of cell viability and ultimately cell death (Sperling *et al.*, 2008). Au NPs have been shown to be non-toxic and biologically inert (Goodman *et al.*, 2004). Gold nanoparticle's ability to cause cytotoxicity depends on their size, shape, functional group, charge, and uptake mechanism by cells (Chen *et al.*, 2009). A549 and MDAMB cancer cell line's IC_{50} for Au NPs was 10 $\mu\text{g/mL}$. 100% of the cells were lysed when the concentration of Au NPs was increased to 30 $\mu\text{g/mL}$. (Asra Parveen and Srinath Rao, 2015).

According to the current study's findings, cell mortality in the HepG2 cell line treated with the phytosynthesized Au NPs at 30 $\mu\text{g/mL}$ reached 51%. The above condition's treatment of the cells resulted in cell shrinkage. Moreover, the cells had apoptotic activity that resulted in cell death as demonstrated by changes in membrane integrity, suppression of cell development, and cytoplasmic condensation (Ashok kumar *et al.*, 2014). The propidium iodide staining technique shows that the cytotoxic effect generated by biosynthesized Au NPs involves apoptotic alterations and nuclear condensation. In the control group, relatively few propidium iodide-positive HepG2 cells were seen. In cells treated with Au NPs at IC_{50} , the proportion of propidium iodide-positive cells gradually increased over the course of 24 hours. Similar to this, cancer cells treated with curcumin or catechin showed enhanced chromatin fluorescence, condensed nuclear shape, and the presence of apoptotic bodies (Manikandan *et al.*, 2012). Ag NPs may cause cell death in MCF7 cells by activating the apoptotic process, which is thought to be mediated by reactive oxygen species. Higher levels of ROS and subsequent loss of mitochondrial membrane potential may be the cause of the enhanced morphological alterations associated with apoptosis in cells exposed to Ag NPs (Piao *et al.*, 2011).

By observing nuclear and cytoplasmic condensation with blebbing that results in the creation and release of apoptotic entities, the induction of apoptosis was examined. The Acridine orange/ethidium bromide (AO/EB) double staining for fluorescence microscopy was used to assess and compare the detection and quantification of necrosis and apoptosis (Vasconcelos and Lam, 1994). In order to discriminate between live, apoptotic, and necrotic cells, this technique combines the differential uptake of fluorescent DNA binding dyes of AO and EB with the morphological aspect of chromatin condensation in the stained nucleus. The AO is absorbed by both living and dead cells, and it displays either green or red fluorescence depending on whether it has intercalated into single-stranded or double-stranded nucleic acids (mostly DNA) (mainly RNA). Only non-viable cells can absorb the EB, and when it intercalates into DNA it exhibits red fluorescence. Therefore a healthy cell has an identical bright green nucleus and an orange cytoplasm. The chromatin of a cell that is on the verge of apoptosis but whose membrane is still intact and which has begun to cleave its DNA is still visible as brilliant green patches due to condensation. The cell still retains a green nucleus. A necrotic cell exhibits a homogenous bright orange nucleus, but a late apoptotic cell exhibits brilliant orange regions of condensed chromatin in the nucleus (EB predominates over AO).

In the current investigation, HepG2 cells treated with Au NPs at IC₅₀ concentration were stained with acridine orange and ethidium bromide after 24 hours. When compared to control cells that had not been treated, they had morphological apoptotic alterations. Normal cell membranes stained with AO showed green fluorescence, whereas apoptotic cells and bodies formed as a result of nuclear blebbing and shrinkage. Their orange-colored bodies were seen to be present. When viewed using a fluorescence microscope, the necrotic cell's loss of membrane integrity was visible as red colour fluorescence (Thangam *et al.*, 2012). Staining with AO and EB revealed the mode of cell death, either from necrotic cell death or from apoptosis. Because AO, a cytoplasmic stain that only stains live cells, became permeable, green fluorescence emission was seen in the untreated tumour cells (Gp2). Whereas DAL cells exposed to Ag NPs displayed reddish orange fluorescence as a result of their lack of membrane integrity (Bhattacharyya *et al.*, 2008).

Endogenous ROS, stochastic mistakes in replication or recombination, as well as environmental toxins, can all cause cellular DNA damage (Asha Rani *et al.*, 2009). The ROS can cause oxidative DNA damage and act as signal molecules driving the advancement of the cell cycle (Allen *et al.*, 1997). DNA fragmentation is widely regarded as an indicator of apoptosis (Wang *et al.*, 2007). DNA fragmentation and irregular cell shrinkage, in which the cells are decreased and shrivelled, are two signs that apoptosis has been triggered (Sriram *et al.*, 2010). Chromosome DNA is cleaved into fragments of oligonucleosomal size as part of the apoptotic process. A significant apoptotic endonuclease for DNA fragmentation *in vitro* was revealed by the elegant biochemical investigation as the DNA fragmentation factor. DNA fragmentation was seen in the current study's HepG2 cells after treatment with Au NPs at the IC₅₀ concentration. Today's manufacturing of multifunctional biogenic nanoparticles is demonstrating impressive impacts, particularly on cancer cells. In a study published in 2019, Banerjee *et al.* investigated the impact of two different cancer cell lines on a physiologically significant peptide, silver (Ag NPs), and gold (Au NPs) nanoparticles in a conjugated form. Under normal circumstances, the peptide (Boc-L-DP-LOMe) was conjugated with biodegradable gold and silver nanoparticles. Both colon cancer (HT-29) and breast cancer (MDA MB- 231) cell lines were used to test these conjugates. The outcomes unmistakably showed that coupled nanoparticles performed better than individual pure nanoparticles in terms of activity. It was demonstrated using fluorescent dye microscopy and a DNA fragmentation assay that conjugated nanoparticles seriously injured cells and render them deadly by significantly fragmenting their DNA.

The traditional chemotherapy used to treat cancer has a number of drawbacks. The development of cancer nanotechnology has opened up new therapeutic options, including medication delivery and nanoformulated therapies. Recently, Haque and Norbet (2021) created Ag NPs (AgZE) derived from *Zinnia elegans* and studied their role in cancer treatments and theranostics on C57BL6/J mice carrying tumours. Using cellular biocompatibility and an NIR-based non-invasive imaging/contrast agent, the concerned AgZE shown effective anti-cancer effects. According to the American Cancer Society, 61,090 new instances of leukaemia had been identified in 2021, and 23,660 people would pass away from this illness in the United States alone (Ebrahim and Atefah, 2022). A void has been formed in society due to its basic requirement for care. Biogenic nanoparticles have emerged as a promising area for the relevant therapies among the several methodologies that have been investigated. In particular, biogenic silver and gold nanoparticles (NPs) with distinctive physiochemical properties have demonstrated effective progression for their anti-leukemic efficacy against cancer

cells. In order to effectively treat leukaemia, it is first necessary to create extremely accurate diagnostic tools. This can be done by producing functionalized NPs for use as contrast agents in bio imaging equipment. The use of NPs in the treatment of cancer has demonstrated its ability to lower undesirable renal clearance, increase the half-life circulation and all-time bioavailability of drugs inside the body, decrease normal tissue exposure to high drug concentrations, and lessen adverse side-effects in the treatment of leukaemia as well as other cancers. Recently, *Spinaciaoleracea* leaf, often known as spinach, was used by Zangeneh *et al.*, (2020) to synthesise Ag NPs that were shown to be antileukemic agents in an animal model of AML while comparing it to the long-term anticancer efficacy of the medication doxorubicin (DOX). More than 13 different types of flavonoids are present in *Spinaciaoleracea* extracts, which may have anticancer and antioxidant properties and are therefore employed as a reducing or capping agent to create Ag NPs. Similar to DOX, green synthetic NPs exhibited potent *in vitro* anticancer activity against a variety of cancer cells, whereas biogenic NPs had no harmful effects on normal cells. *Hibiscus sabdariffa* (roselle), according to Zangenehet *al.*, (2020), is essential for the production of Au NPs. The extract has great qualities including selective cytotoxicity, apoptosis, cell cycle arrest, anti-metastatic, and autophagy actions against many types of human cancer cells because of the higher levels of polyphenolic compounds present in it.

5. CONCLUSION

The present study demonstrates the potential of *Ulva fasciata* as a sustainable and eco-friendly biological system for the green synthesis of gold nanoparticles. Utilizing naturally occurring phytochemicals within the seaweed extract, the synthesis process avoids the need for harmful chemicals or high-energy inputs, aligning with the principles of green chemistry. The biological molecules within the extract act both as reducing and stabilizing agents, enabling the formation of nanoparticles with desirable physicochemical characteristics. Furthermore, the study supports the growing interest in marine resources as a valuable and renewable source for nanomaterial production. Given their biogenic origin, such nanoparticles are particularly promising for applications in biomedicine, especially in the development of safer therapeutic agents. This approach underscores the integration of natural resources and nanotechnology for innovative, environmentally responsible applications in science and healthcare.

COMPETING INTERESTS DISCLAIMER:

Authors have declared that they have no known competing financial interests OR non-financial interests OR personal relationships that could have appeared to influence the work reported in this paper.

REFERENCES

Aggarwal, R., Sheikh, A., Akhtar, M., Ghazwani, M., Hani, U., Sahebkar, A., et al. (2025). Understanding gold nanoparticles and their attributes in ovarian cancer therapy. *Molecular Cancer*, 24(1), 88.

<https://doi.org/10.1186/s12943-025-02280-3>

Allen, R. T., Hunter, W. J., & Agrawal, D. K. (1997). Morphological and biochemical characterization and analysis of apoptosis. *Journal of Pharmacological and Toxicological Methods*, 37(4), 215–228. [https://doi.org/10.1016/S1056-8719\(97\)00033-6](https://doi.org/10.1016/S1056-8719(97)00033-6)

AshaRani, P. V., Hande, M. P., & Valiyaveetil, S. (2009). Anti-proliferative activity of silver nanoparticles. *BMC Cell Biology*, 10, 65.

<https://doi.org/10.1186/1471-2121-10-65>

Ashokkumar, T., Prabhu, D., Geethaa, R., Govindaraju, K., Manikandan, R., Arulvasu, C., et al. (2014). Apoptosis in liver cancer (HepG2) cells induced by functionalized gold nanoparticles. *Colloids and Surfaces B: Biointerfaces*, 123, 549–556. <https://doi.org/10.1016/j.colsurfb.2014.09.051>

Parveen, A., & Rao, S. (2015). Cytotoxicity and genotoxicity of biosynthesized gold and silver nanoparticles on human cancer cell lines. *Journal of Cluster Science*, 26(3), 775–788. <https://doi.org/10.1007/s10876-014-0810-6>

Banerjee, K., Ravishankar Rai, V., & Umashankar, M. (2019). Effect of peptide-conjugated nanoparticles on cell lines. *Progress in Biomaterials*, 8(1), 11–21.

<https://doi.org/10.1007/s40204-019-0106-9>

Bhattacharyya, S. S., Mandal, S. K., Biswas, R., Paul, S., Pathak, S., Boujedaini, N., et al. (2008). In vitro studies demonstrate anticancer activity of an alkaloid of the plant *Gelsemium sempervirens*. *Experimental Biology and Medicine*, 233(12), 1591–1601.

<https://doi.org/10.3181/0805-RM-181>

Bloise, N., Strada, S., Dacarro, G., & Visai, L. (2022). Gold nanoparticles contact with cancer cell: A brief update. *International Journal of Molecular Sciences*, 23(14), 7683. <https://doi.org/10.3390/ijms23147683>

Boisselier, E., & Astruc, D. (2009). Gold nanoparticles in nanomedicine: preparations, imaging, diagnostics, therapies and toxicity. *Chemical Society Reviews*, 38(6), 1759–1782. <https://doi.org/10.1039/B806051G>

Brown, S. D., Nativo, P., Smith, J. A., Stirling, D., Edwards, P. R., Venugopal, B., et al. (2010). Gold nanoparticles for the improved anticancer drug delivery of the active component of oxaliplatin. *Journal of the American Chemical Society*, 132(13), 4678–4684.

<https://doi.org/10.1021/ja910270m>

Chen, Y. S., Hung, Y. C., Liao, I., & Huang, G. S. (2009). Assessment of the in vivo toxicity of gold nanoparticles. *Nanoscale Research Letters*, 4(8), 858–864.

<https://doi.org/10.1007/s11671-009-9327-8>

Ebrahim, M., Atefah, Z., Barabadi, H., Zarrabi, A., Truong, L. B., & Medina-Cruz, D. (2022). Antineoplastic activity of biogenic silver and gold nanoparticles to combat leukemia: Beginning a new era in cancer theragnostic. *Biotechnology Reports*, 34, e00714. <https://doi.org/10.1016/j.btre.2022.e00714>

Edlund, U., & Albertsson, A. C. (2003). Polyesters based on diacid monomers. *Advanced Drug Delivery Reviews*, 55(4), 585–609.

[https://doi.org/10.1016/S0169-409X\(03\)00042-0](https://doi.org/10.1016/S0169-409X(03)00042-0)

Evans, W. C. (1997). *Trease and Evans Pharmacognosy* (14th ed.). Singapore: Harcourt Brace and Company.

Gahan, P. B. (1984). *Plant Histochemistry and Cytochemistry: An Introduction*. London, New York: Academic Press.

Ghosh, P., Han, G., De, M., Kim, C. H., & Rotello, V. M. (2008). Gold nanoparticles in delivery applications. *Advanced Drug Delivery Reviews*, 60(11), 1307–1315. <https://doi.org/10.1016/j.addr.2008.03.016>

Goodman, C. M., McCusker, C. D., Yilmaz, T., & Rotello, V. M. (2004). Toxicity of gold nanoparticles functionalized with cationic and anionic side chains. *Bioconjugate Chemistry*, 15(4), 897–900. <https://doi.org/10.1021/bc049951i>

Haque, S., Norbert, C. C., Acharyya, R., Mukherjee, S., Kathirvel, M., & Patra, C. R. (2021). Biosynthesized silver nanoparticles for cancer therapy and in vivo bioimaging. *Cancers*, 13(23), 6114. <https://doi.org/10.3390/cancers13236114>

Hirak, K., Patra, S., Banerjee, S., Chaudhuri, U., Lahiri, P., Anjan, K. R., & Dasgupta, S. (2007). Cell selective response to gold nanoparticles. *Nanomedicine: Nanotechnology, Biology and Medicine*, 3(2), 111–119.

<https://doi.org/10.1016/j.nano.2007.02.005>

Hossain, A., Rayhan, M. T., Mobarak, M. H., Rimon, M. I. H., Hossain, N., Islam, S., & Kafi, S. M. A. (2024). Advances and significances of gold nanoparticles in cancer treatment: A comprehensive review. *Results in Chemistry*, 8, 101559.

<https://doi.org/10.1016/j.rechem.2023.101559>

Jayshree, N., Cynthia, P., & Kanchana, A. (2012). Biogenic synthesis by *Sphearanthusamaranthoids*; towards the efficient production of biocompatible gold nanoparticles. *Digest Journal of Nanomaterials and Biostructures*, 7(1), 123–133.

Jeyaraj, M., Rajesh, M., Arun, R., Ali, M., Sathishkumar, G., Sivanandhan, G., et al. (2013). An investigation on the cytotoxicity and caspase-mediated apoptotic effect of biologically synthesized silver nanoparticles using *Podophyllumhexandrum* on human cervical carcinoma cells. *Colloids and Surfaces B: Biointerfaces*, 102, 708–717.

<https://doi.org/10.1016/j.colsurfb.2012.09.044>

Jiang, W., Kim, B. Y. S., Rutka, J. T., & Chan, W. C. W. (2008). Nanoparticle-mediated cellular response is size-dependent. *Nature Nanotechnology*, 3(3), 145–150. <https://doi.org/10.1038/nnano.2008.30>

Khan, A. K., Rashid, R., Murtaza, G., & Zahra, A. (2014). Gold nanoparticles: Synthesis and applications in drug delivery. *Tropical Journal of Pharmaceutical Research*, 13(7), 1169–1177. <https://doi.org/10.4314/tjpr.v13i7.23>

Kisak, E. T., Coldren, B., Evans, C. A., Boyer, C., & Zasadzinski, J. A. (2004). The vesosome – a multicompartiment drug delivery vehicle. *Current Medicinal Chemistry*, 11, 199–219. <https://doi.org/10.2174/0929867043365096>

Kokate, C. K. (1999). *Practical pharmacognosy* (4th ed.). New Delhi, India: Vallabhprakashan Publications.

Mace, M. (1963). Histochemical localization of phenols in healthy and diseased banana roots. *Physiologia Plantarum*, 16(4), 915–925.

<https://doi.org/10.1111/j.1399-3054.1963.tb07014.x>

Manikandan, R., Beulaja, M., Arulvasu, C., Sellamuthu, S., Dinesh, D., Prabhu, D., et al. (2012). Synergistic anticancer activity of curcumin and catechin: An in vitro study using human cancer cell lines. *Microscopy Research and Technique*, 75(1), 112-116.

<https://doi.org/10.1002/jemt.20940>

Mohammadi, H., Abedi, A., Akbarzadeh, A., Mokhtari, M. J., Shahmabadi, H. E., Mehrabi, M., et al. (2013). Evaluation of synthesized platinum nanoparticles on the MCF-7 and HepG-2 cancer cell lines. *Nano Letters*, 3, 1-28.

Mosmann, T. (1983). Rapid colorimetric assay for cellular growth and survival: application to proliferation and cytotoxicity assays. *Journal of Immunological Methods*, 65(1-2), 55-63.

[https://doi.org/10.1016/0022-1759\(83\)90303-4](https://doi.org/10.1016/0022-1759(83)90303-4)

Mubarak Ali, D., Thajuddin, N., Jeganathan, K., & Gunasekaran, M. (2011). Plant extract mediated synthesis of silver and gold nanoparticles and its antibacterial activity against clinically isolated pathogens. *Colloids and Surfaces B: Biointerfaces*, 85(2), 360-365.

<https://doi.org/10.1016/j.colsurfb.2011.06.007>

Nisha, Sachan, R. S. K., Singh, A., Karnwal, A., Shidiki, A., & Kumar, G. (2024). Plant-mediated gold nanoparticles in cancer therapy: exploring anticancer mechanisms, drug delivery applications, and future prospects. *Frontiers in Nanotechnology*, 6, 1490980. <https://doi.org/10.3389/fnano.2024.1490980>

Pan, Y., Neuss, S., Leifert, A., Fischler, M., & Wen, F. (2012). Size-dependent cytotoxicity of gold nanoparticles. *Nano Small Micro*, 3(11), 1941-1949.

<https://doi.org/10.1002/sml.201200783>

Piao, M. J., Kang, K. A., & Lee, I. K. (2011). Silver nanoparticles induce oxidative cell damage in human liver cells through inhibition of reduced glutathione and induction of mitochondria-involved apoptosis. *Toxicology Letters*, 201(1), 92-100.

<https://doi.org/10.1016/j.toxlet.2010.11.020>

Ramakrishna, S., Prasanan, K. G., & Rajan, R. (1994). *Textbook of medicinal biochemistry*. New Delhi, India: Orient Longman.

Salem, A. K., Searson, P. C., & Leong, K. W. (2003). Multifunctional nanorods for gene delivery. *Nature Materials*, 2(9), 668-671.

<https://doi.org/10.1038/nmat983>

Sathishkumar, M., Sneha, K., & Won, S. W. (2009). Cinnamon zeylanicum bark extract and powder mediated green synthesis of nanocrystalline silver particles and its bactericidal activity. *Colloids and Surfaces B: Biointerfaces*, 73(2), 332-338.

<https://doi.org/10.1016/j.colsurfb.2009.05.007>

Shukla, R., Bansal, V., Chaudhary, M., Basu, A., Bhonde, R. R., & Sastry, M. (2005). Biocompatibility of gold nanoparticles and their endocytotic fate inside the cellular compartment: a microscopic overview. *Langmuir*, 21(23), 10644-10654.

<https://doi.org/10.1021/la051927r>

Singh, M., Kumar, M., Manikandan, S., Chandrasekaran, N., Mukherjee, A., & Kumaraguru, (2014). Drug delivery system for controlled cancer therapy using physico chemically stabilized bioconjugated gold nanoparticles synthesized from marine macroalgae, *Padinagymnospora*. *Journal of Nanomedicine & Nanotechnology*, 5(2), 2-7.

<https://doi.org/10.4172/2157-7439.1000195>

Sperling, R. A., Rivera Gil, P., Zhang, F., Zanella, M., & Parak, W. J. (2008). Biological applications of gold nanoparticles. *Chemical Society Reviews*, 37(9), 1896-1908.

<https://doi.org/10.1039/b710782b>

Sriram, M. I., Kanth, S. B., Kalishwaralal, K., & Gurunathan, S. (2010). Antitumor activity of silver nanoparticles in Dalton's lymphoma ascites tumor model. *International Journal of Nanomedicine*, 5, 753-762.

<https://doi.org/10.2147/IJN.S11388>

Thangam, R., Gunasekaran, P., Kaveri, K., Sridevi, G., Sundarraj, S., & Paulpandi, M. (2012). A novel disintegrin protein from *Naja naja* venom induces cytotoxicity and apoptosis in human cancer cell lines in vitro. *Process Biochemistry*, 47(8), 1243-1249.

<https://doi.org/10.1016/j.procbio.2012.05.021>

Torresdey, G. J. L., Parsons, J. G., Gomez, E., Peralta-Videa, J., Troiani, H. E., Santiago, P., et al. (2003). Alfalfa sprouts: A natural source for the synthesis of silver nanoparticles. *Langmuir*, 19(4), 1357-1361.

<https://doi.org/10.1021/la0268226>

Vasconcelos, A. C., & Lam, K. M. (1994). Apoptosis induced by infectious bursal disease virus. *Journal of General Virology*, 75(7), 1803-1806.

<https://doi.org/10.1099/0022-1317-75-7-1803>

Verma, S., Abirami, S., & Mahalakshmi, S. (2013). Anticancer and antibacterial activity of silver nanoparticles biosynthesized by *Penicillium* spp. and its synergistic effect with antibiotics. *Journal of Microbiology and Biotechnology Research*, 3(3), 54-71.

Vines, J. B., Yoon, J. H., Ryu, N. E., Lim, D. J., & Park, H. (2019). Gold nanoparticles for photothermal cancer therapy. *Frontiers in Chemistry*, 7, 167. <https://doi.org/10.3389/fchem.2019.00167>

Wagner, H. (1993). *Pharmazeutische Biologie. Drogen und ihre Inhaltsstoffe*. New York: Gustav Fischer Verlag.

Wagner, H. X. S., Blatt, Z., & Gain, E. M. (1996). *Plant Drug Analysis*. Berlin, Germany: Springer.

Wang, M. D., Shin, D. M., Simons, J. W., & Nie, S. (2007). Nanotechnology for targeted cancer therapy. *Expert Review of Anticancer Therapy*, 7(6), 833-837. <https://doi.org/10.1586/14737140.7.6.833>

Wu, W., Wieckowski, S., Pastorin, G., Benincasa, M., Klumpp, C., Briand, J. P., et al. (2005). Targeted delivery of amphotericin B to cells by using functionalized carbon nanotubes. *Angewandte Chemie International Edition*, 44(41), 6358-6362.

<https://doi.org/10.1002/anie.200501312>

Yasuma, A., & Ichikawa, T. (1953).Ninhydrin-Schiff and Alloxan-Schiff staining: A new histochemical staining method for protein. *The Journal of Laboratory and Clinical Medicine*, 41(2), 296-299.

Zangeneh, M. M. (2020). Synthesis and formulation of a modern chemotherapeutic drug of *Spinaciaoleracea* L. leaf aqueous extract conjugated silver nanoparticles: Chemical characterization and analysis of their cytotoxicity, antioxidant, and anti-acute myeloid leukemia properties in comparison to doxorubicin in a leukemic mouse model. *Applied Organometallic Chemistry*, 34(1), e5295. <https://doi.org/10.1002/aoc.5295>

UNDER PEER REVIEW

UNDER PEER REVIEW